Pergamon

Tetrahedron 57 (2001) 4567–4578

TETRAHEDRON

Chiral discrimination of permethylated *gluco*-oligosaccharide toward amino acid ester salts

Motohiro Shizuma,[a,*] Hiroshi Adachi,[b] Akinori Amemura,[c] Yoshio Takai,[d] Tokuji Takeda[a] and Masami Sawada[d,*]

[a]*Osaka Municipal Technical Research Institute, 1-6-50 Morinomiya, Joto-ku, Osaka 536-8553, Japan*
[b]*Faculty of Science, Osaka University, 1-1 Machikaneyama, Toyonaka, Osaka 560-0043, Japan*
[c]*Faculty of Engineering, Fukuyama University, Sanzo 1 Gakuen-cho, Fukuyama, Hiroshima 729-0292, Japan*
[d]*Materials Analysis Center, The Institute of Scientific and Industrial Research, Osaka University, 8-1 Mihogaoka, Ibaraki, Osaka 567-0047, Japan*

Received 14 March 2001; accepted 4 April 2001

Abstract—The chiral discrimination ability of permethylated glucopyrano-oligosaccharides toward amino acid 2-propyl ester hydrochlorides was evaluated using FAB mass spectrometry. In the given permethylated homo-oligosaccharides, permethylated β-cello-oligosaccharide series (II) showed remarkably higher *S*-selectivity toward tryptophan ester salts (Trp-O-*i*Pr$^+$) independent of the numbers (n) of the glucopyranose unit (n=2–5). The hexamer and heptamer of the permethylated β-malto-oligosaccharide series (I) showed the very similar enantioselectivity to permethylated α- and β-cyclodextrin. © 2001 Elsevier Science Ltd. All rights reserved.

1. Introduction

Carbohydrates play important roles in the molecular recognition processes of living systems using the complicated structures found in stereochemistry. Molecular recognition in living systems involves chiral recognition, which is a significant and fundamental process. Carbohydrates, polysaccharides and their derivatives have chiral discrimination ability and this is applied to the chiral stationary phase in liquid chromatography.[1] Chiral discrimination of some linear oligosaccharides toward chiral compounds has been reported.[2] However, there are few studies on the 1:1 enantioselective complexation of oligosaccharides and their derivatives with chiral compounds.[3] In this study we clarify the 1:1 enantioselective complexation characteristics of oligosaccharide derivatives with chiral organic ammoniums using FAB mass spectrometry.[4]

In the present article, we report on the chiral discrimination ability of five permethylated glucopyrano-oligosaccharide series (Scheme 1) [β-malto-oligosaccharides (β-MeMal(n), n=2–7, series I), β-cello-oligosaccharides (β-MeCel(n), n=2–5, series II), α-laminari-oligosaccharides (α-MeLam(n), n=2–5, series III-α), β-laminari-oligosaccharides (β-MeLam (n), n=2–5, series III-β), and isomalto-oligosaccharides (β-MeImal(n), n=2–7, series IV)] toward seven species of amino acid 2-propyl ester hydrochlorides (Scheme 2), which was evaluated using FAB mass spectrometry. It was found that the β-MeCel(n) values show remarkably higher enantioselectivity toward Trp-O-*i*Pr$^+$. It is very interesting that the influence of the glucosyl bond style on the chiral discrimination ability is very different among the series I, II, III and IV.

2. Results and discussion

2.1. Chiral discrimination

The chiral discrimination ability was evaluated by means of a FAB mass spectrometry (MS)/enantiomer labeled (EL) guest method (Table 1).[5] In this method, FAB mass spectra of permethylated oligosaccharide (S) and a 1:1 deuterium-labeled/unlabeled enantiomeric mixture of the amino acid ester salts (G_{S-dx}^+ and G_R^+) in 3-nitrobenzyl alcohol (NBA) matrix were measured and the peak intensity of two complex ions [$(S+G_R)^+$ and $(S+G_{S-dx})^+$] of the saccharide with each enantiomer of amino acid ester salt was observed in the spectra. The complex ion peaks differ about the m/z (equal to x, where x is the number of deuteriums) by the labeling with the deuterium. The chiral discrimination ability of the saccharides is evaluated by the relative peak intensity $[I(S+G_R)^+/I(S+G_{S-dx})^+=I_R/I_{S-dx}]$ values. The details of this method have been already reported and reviewed by others.[6] In electrospray ionization (ESI) mass

Keywords: amino acids and derivatives; carbohydrate; enantioselection; molecular recognition.
* Corresponding authors. Fax: +81-6-6963-8040; e-mail: shizuma@omtri.city.osaka.jp

0040–4020/01/$ - see front matter
PII: S0040-4020(01)00390-8

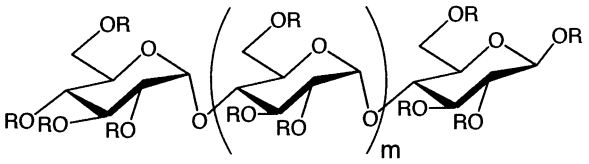

I β-Malto-oligosaccharides

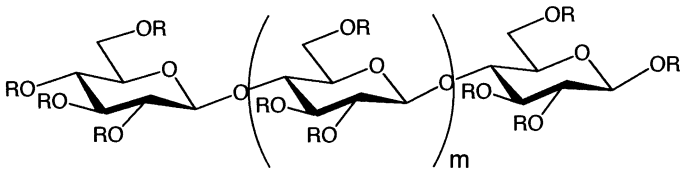

II β-Cello-oligosaccharides

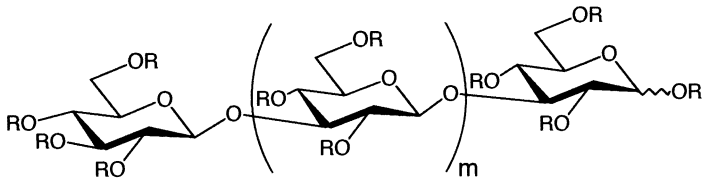

III-α **III-β** α- and β-liminari-oligosaccharides

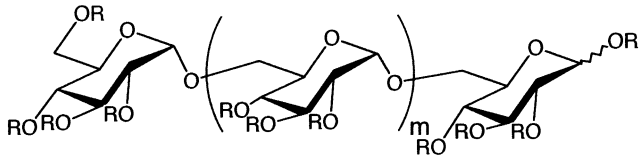

IV Isomalto-oligosaccharides

I, β-MeMal (n), m = 0 ~ 5; **II**, β-MeCel (n), m = 0 ~ 3; **III-α**, α-MeLam (n), m = 0 ~3;
III-b, β-MeLam (n), m = 0 ~ 3; **IV**, MeImal (n), m = 0 ~ 5. n = m + 2.

Scheme 1. Permethylated *gluco*-oligosaccharides (R=CH_3).

spectrometry, various complex ions are easily and directly detected from a given sample solution. However, the chiral discrimination ability evaluated by ESIMS was decreased in comparison with that by FABMS.[7] For the above reason, the FABMS method was adopted for the evaluation.

The FAB mass spectra of the permethylated penta-oligosaccharides in the present series with Trp-O-*i*$Pr^+(Cl^-)$ are shown in Fig. 1. The diastereomeric 1:1 complex ions were observed in the given saccharides and the amino acid ester hydrochloride pair. In the case of series I, the chiral discrimination was slightly detected toward Trp-O-*i*Pr^+ and Pro-O-*i*Pr^+ (*R*-selectivity). In the case of series III, the chiral discrimination ability was very small. In series IV, the chiral discrimination was hardly observed except in the case of MeImal2 toward Trp-O-*i*Pr^+ (I_R/I_{S-dx}=0.65, *S*-selectivity). Especially in the case of series II, the chiral discrimination toward Trp-O-*i*Pr^+ was clearly detected (Fig. 2). The chiral discrimination ability was larger than the combination of the other series and the amino acid derivatives. The ability hardly depends on the numbers of the glucopyranose units in series II, i.e. I_R/I_{S-dx} is roughly constant at 0.6–0.5 for β-MeCel2–β-MeCel5. The disaccharide MeCel2 in the series showed relatively higher chiral discrimination ability. It is then suggested that the binding site comprises the next glucopyranose unit to each other. Note also that the permethylated β-D-glucopyranose (monosaccharide) showed no chiral discrimination ability toward all given amino acid ester hydrochlorides (Table 1), supporting the above observation that two glucose units are necessary for chiral discrimination.

2.2. Molecular dynamics of penta-oligosaccharides

The dynamic structures of the permethylated penta-oligosaccharides were simulated using the molecular dynamics (MD) program. The most stable structure of the linear saccharides is not easy to determine by molecular simulation methods such as the molecular orbital (MO) and the molecular mechanics (MM) calculations because

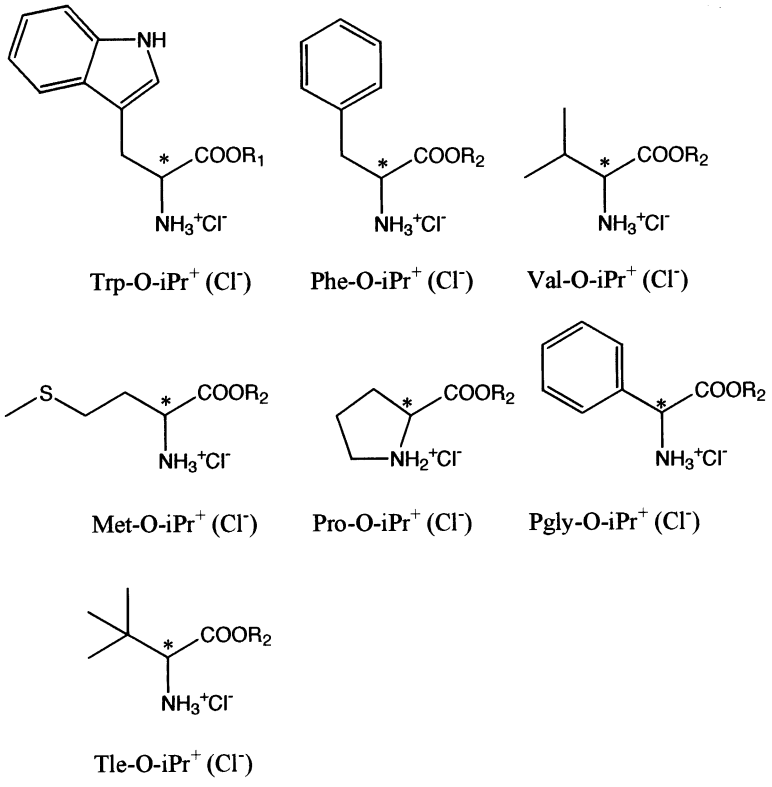

Scheme 2. Labeled/unlabeled amino acid 2-propyl ester hydrochloride pairs. (*R*)-Enantiomer: R_1=R_2=$CH(CH_3)_2$; (*S*)-enantiomer: R_1=$CH(CD_3)_2$ [d_6]; R_2=$CD(CD_3)_2$, [d_7].

Table 1. Chiral discrimination ability (I_R/I_{S-dx} values) of permethylated *gluco*-oligosaccharides toward amino acid 2-propyl esters in FAB mass spectrometry

Permethylated oligosaccharides		Trp	Phe	Val	Met	Pro	Pgly	Tle
I	β-MeMal2	1.06	1.06	0.96	1.07	1.16	0.98	0.95
	β-MeMal3	1.12	1.05	0.97	1.12	1.07	0.91	0.95
	β-MeMal4	1.13	1.02	1.01	1.08	1.08	0.91	0.99
	β-MeMal5	1.15	1.01	0.98	1.08	1.07	0.86	0.95
	β-MeMal6	1.17	1.06	1.02	1.08	1.17	0.87	0.92
	β-MeMal7	1.14	1.01	1.03	1.15	1.08	0.86	0.97
II	β-MeCel2	0.62	0.97	1.00	1.04	0.94	0.90	0.97
	β-MeCel3	0.57	1.01	0.97	1.00	1.09	0.91	0.98
	β-MeCel4	0.59	0.98	0.98	0.97	1.08	0.89	0.95
	β-MeCel5	0.49	0.96	0.93	0.98	1.06	0.89	1.05
III-α	α-MeLam2	0.92	0.99	0.97	1.00	1.07	0.93	0.89
	α-MeLam3	0.86	1.00	1.04	1.02	1.07	0.97	0.97
	α-MeLam4	0.84	0.97	0.96	1.01	1.08	0.93	0.95
	α-MeLam5	0.83	0.97	0.97	0.99	1.17	0.96	0.98
III-β	β-MeLam2	0.98	1.05	0.97	1.00	1.07	0.99	0.92
	β-MeLam3	0.88	1.03	1.07	1.12	1.09	1.01	0.98
	β-MeLam4	0.78	1.02	1.01	1.07	1.06	0.98	0.99
	β-MeLam5	0.79	0.96	0.97	1.01	1.16	0.96	0.91
IV	MeImal2	0.65	0.79	0.82		0.91	0.85	0.87
	MeImal3	1.01	0.91	0.90		1.12	0.93	0.87
	MeImal4	0.86	0.96	0.93		1.11	0.92	0.90
	MeImal5	0.96	0.92	0.93		1.09	0.90	0.92
	MeImal6	0.98	0.93	0.94		1.17	0.87	0.95
	MeImal7	1.04	0.95	0.96		1.15	0.84	1.00
	β-MeGlc	1.01	1.03	1.01	0.98	1.05	0.96	0.99
Ref.	18-crown-6	1.01	0.99	0.99	0.99	0.99	0.99	0.98

of the flexibility of conformations like chains. So, the MD was applied in order to evaluate the average structure of the various conformations. The dynamic properties expected by the MD simulation are summarized in Table 2. The expected self-diffusion coefficients, which are concerned with the size and the shape of the molecules, for β-MeCel5 and β-MeLam5 were larger than that for β-MeMal5. For the averaged distance from C-1 of the methoxy group in the reducing terminal to the C-4 of the methoxy group in the irreducing terminal (*L*), and the averaged radius of gyration, β-MeCel5 was also larger than β-MeMal5. The above expected properties determined by

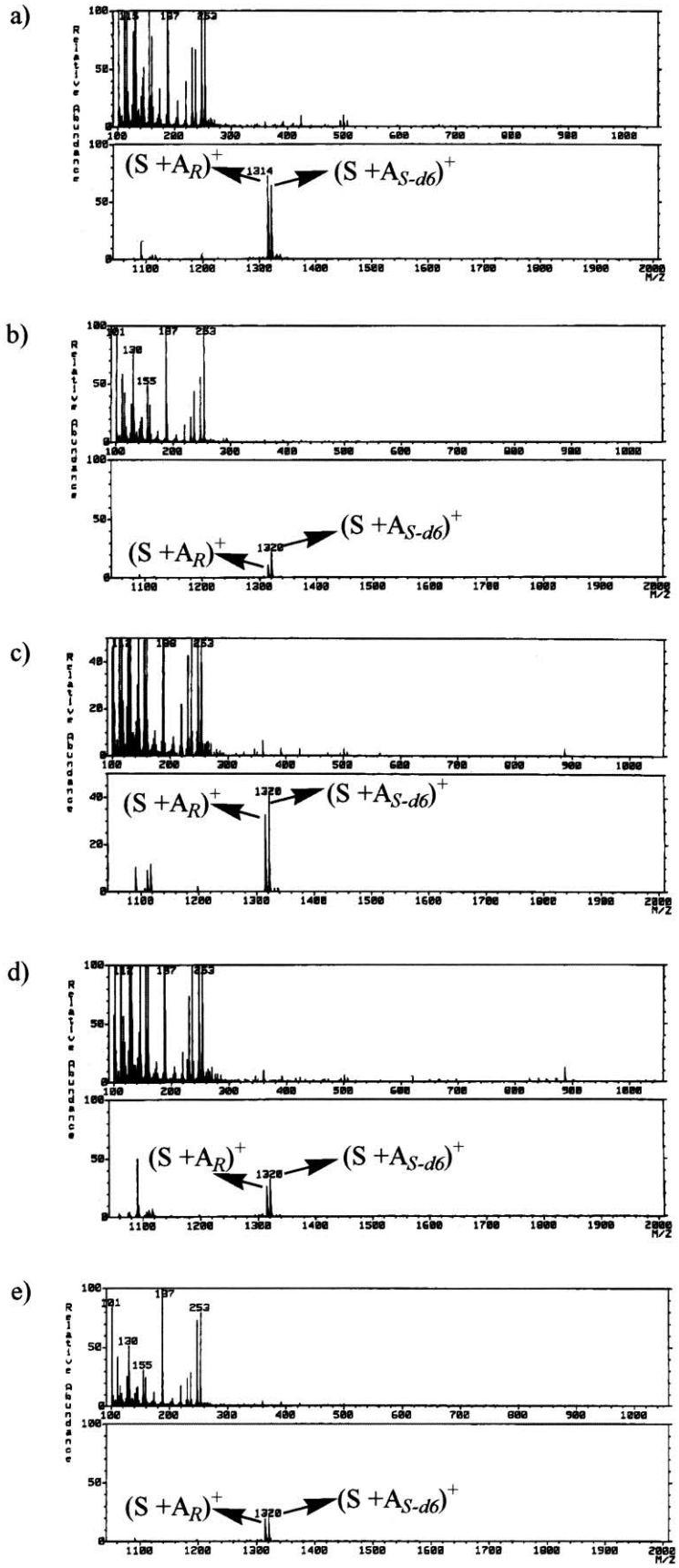

Figure 1. FAB mass spectra of permethylated penta-oligosaccharides with Trp-O-*i*Pr$^+$: (a) β-MeMal5; (b) β-MeCel5; (c) α-MeLam5; (d) β-MeLam5; (e) MeImal5.

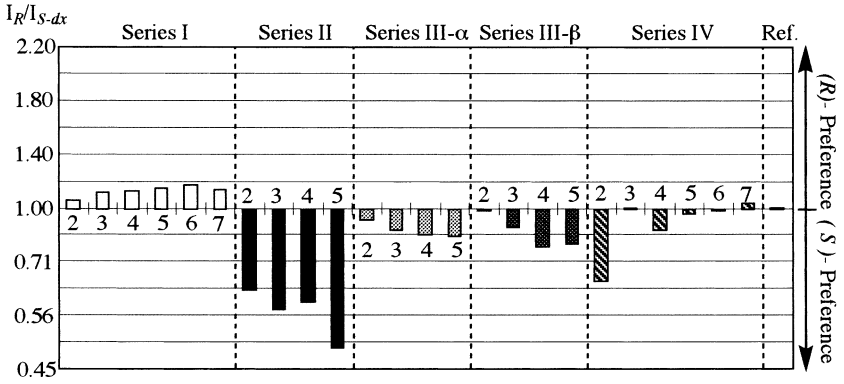

Figure 2. Chiral discrimination ability (I_R/I_{S-dx} values) of permethyl *gluco*-oligosaccharides toward Trp-O-*i*Pr$^+$. 18-crown-6, which is an achiral host, was used as the standerd reference (Ref.).

Table 2. Properties of permethylated penta-oligosaccharides calculated by molecular dynamics

Penta-oligosaccharides	Self-diffusion coefficient ($cm^2\ s^{-1}\ atom^{-1}$)	Distance (L)[a] (Å)	Radius of gyration (Å)
β-MeMal5	0.955×10^{-6}	12.7	5.70
β-MeCel5	0.254×10^{-7}	23.1	7.97
β-MeLam5	0.366×10^{-7}	19.7	7.37
β-MeImal5	0.177×10^{-6}	21.7	6.63

[a] L: the averaged distance from C-1 of the methoxy group in the reducing terminal to C-4 of the methoxy group in the irreducing terminal.

the MD simulation corresponds with those of β-MeCel5 having the linear-type structure and β-MeMal5 having the pseudo-ring-type structure (Fig. 3). The structure of the free (uncomplexed) permethylated oligosaccharides is not necessarily the same as that of the complexes. However, the free structure seems to be referable to the complex structure, especially to the binding site.

2.3. Comparison between the β-MeMal series and the permethylated cyclodextrin series

Because the β-MeMal5 was expected to be a pseudo-ring structure by the MD simulation, it is reasonably assumed that β-MeMal6 and β-MeMal7 have similar pseudo-ring structures. On the other hand, the complex structure of

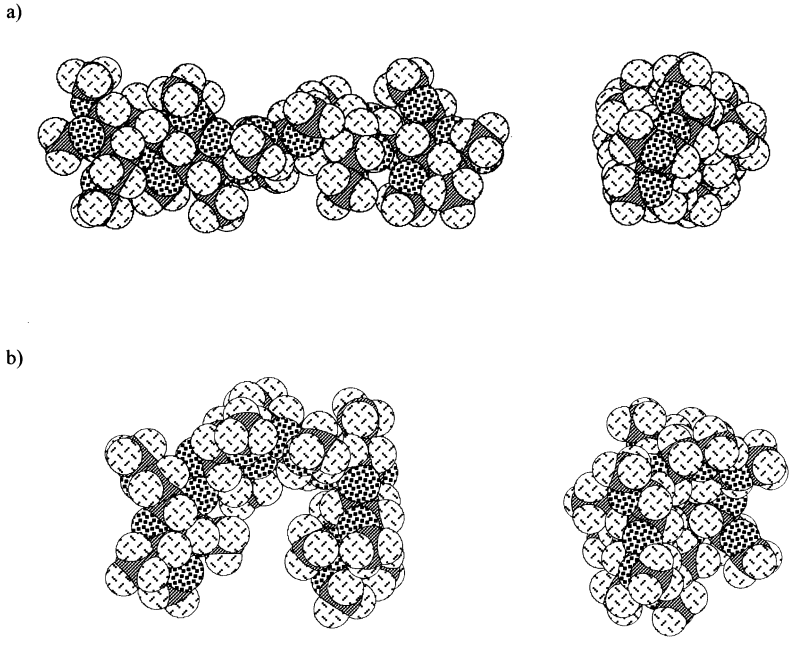

Figure 3. Averaged molecular structure of permethylated penta-oligosaccharides expected by molecular simulation: (a) β-MeCel5; (b) β-MeMal5.

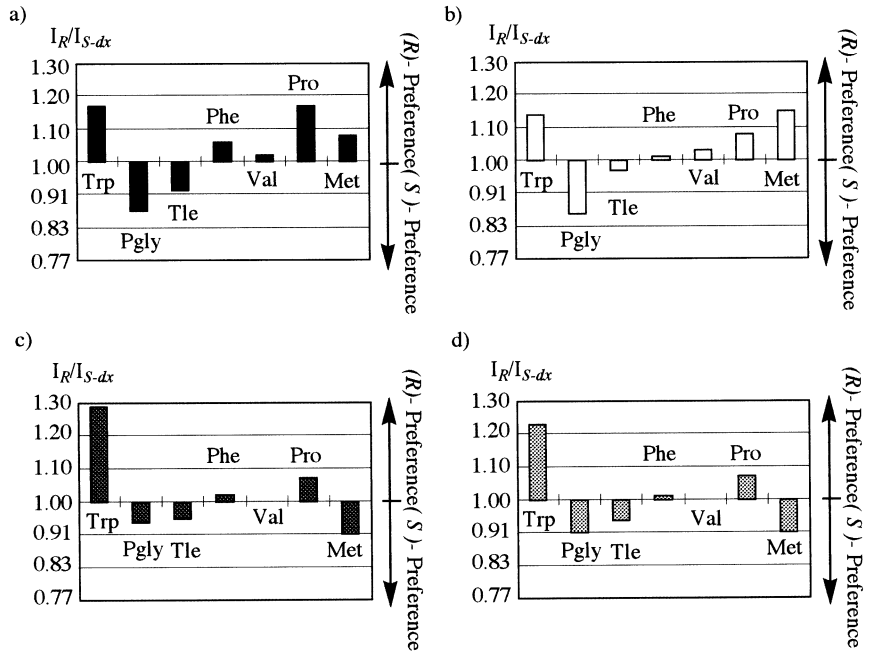

Figure 4. Comparison of the I_R/I_{S-dx} values of β-MeMal(n) (n=6 and 7) and those of permethylated cyclodextrin [MeCD(n)] (n=6 and 7) in terms of chiral discrimination toward amino acid 2-propyl ester hydrochlorides: (a) MeMal6; (b) MeMal7; (c) MeCD6; and (d) MeCD7.

cyclodextrin—which has a cyclic structure consisting of α(1→4)-linked glucopyranose units—with tryptophan has been studied in detail by Lipkowitz et al.[8] In that study, the indole moiety of the tryptophan locates in the hole of α-cyclodextrin, and the functional groups in the tryptophan such as the amino group and the carboxylic group interact with the oxygens of the carbohydrate. The complex of the α-cyclodextrin with (*R*)-tryptophan was assumed to be more stable than the complex with (*S*)-tryptophan. The chiral discrimination of permethylated cyclodextrins (α-MeCD and β-MeCD) toward some amino acid ester salts has been previously reported.[4] Also, the MeCD series did not show any remarkable chiral discrimination ability as in β-MeMal(n). However, the chiral discrimination of the MeCD series is characteristically in good agreement with the chiral discrimination of series I oligosaccharides except in the case toward Met-O-iPr$^+$ (Fig. 4). The good agreement suggests that the binding site of series I structures is the same as that of cyclodextrins although the structure cannot be confirmed yet using the spectrometric method. The

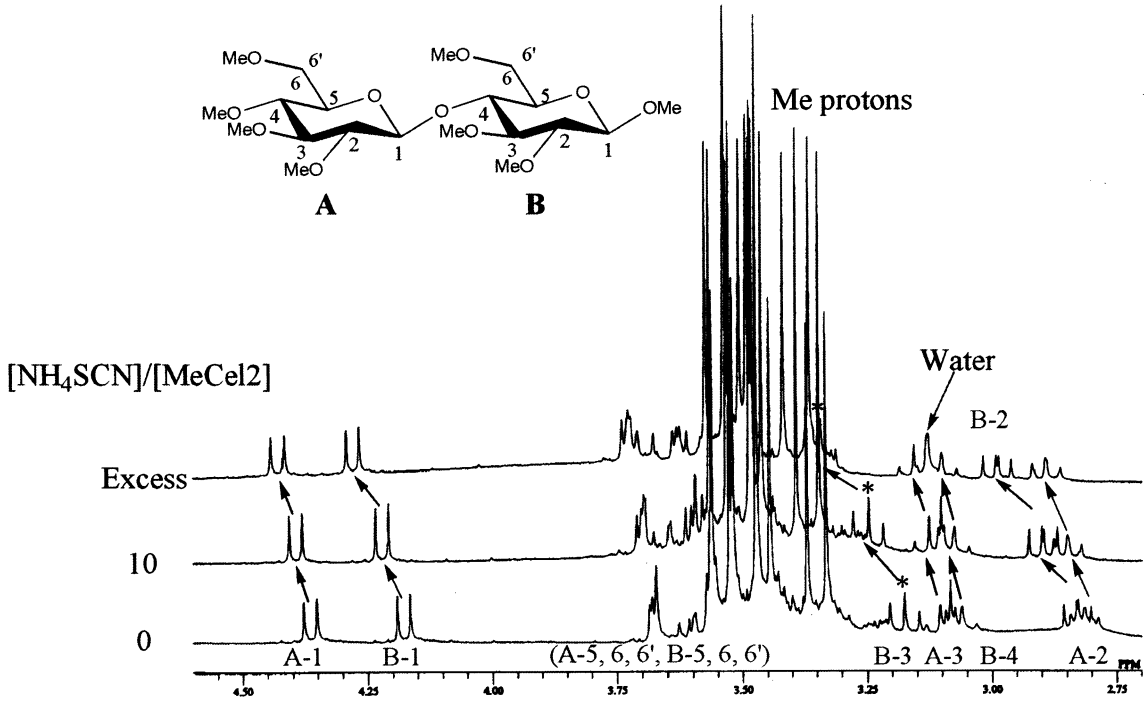

Figure 5. ^{1}H-NMR spectra of β-MeCel2 adding NH_4SCN in acetone-d_6 at 298 K. In the case of [NH_4SCN]/[β-MeCel2]=0, [β-MeCel2]=0.00865 M.

complex structure of β-MeMal(*n*) molecules is not easily clarified because of the small spectral change induced by the complexation compared with cyclodextrins.

2.4. Expected complex structure of series II molecules with Trp-O-*i*Pr$^+$

In order to clarify the binding site of the cationic moiety (NH_3^+) of Trp-O-*i*Pr$^+$ in the complex with β-MeCel2, the ^{1}H-NMR-induced shifts of β-MeCel2 that occur when adding $NH_4^+(SCN^-)$ were followed in acetone-d_6 at 25°C (Fig. 5).[9] For facile observation of the induced shifts, an ammonium ion was used in order to omit the redundant interaction such as the π-effect of the indole moiety of Trp-O-*i*Pr$^+$ etc. Acetone-d_6 was selected as the solvent because of the solvent effect which enhances the electrostatic interaction with the cation and the solubility of ammonium thiocyanate. The specific induced shifts of the pyranose ring protons were observed. Especially, the B-3 proton showed larger down-field shifts in its signal (0.16 ppm). Therefore, ammonium would bind mainly to the oxygen of the OMe-3 group.[10] The 1:1 association constant was evaluated at ca. 1 M^{-1} from the induced shifts.

Further, for clarifying the interaction between β-MeCel2 and the indole moiety of Trp-O-*i*Pr$^+$, ^{1}H-NMR spectra of β-MeCel2 were measured while adding (*S*)-Trp-O-*i*Pr$^+$ in D_2O at 25°C (Fig. 6). Here, D_2O was selected as the solvent in order to enhance the electrophobic interaction such as the CH–π interaction: generally, the CH–π interaction, for example, between β-MeCel2 and the indole moiety of Trp-O-*i*Pr$^+$ in the complex,would be enhanced in the gas phase. Most of the peaks showed slight down-field shifts or no shift. One of the OMe groups showed a small up-field shift (0.02 ppm) by the π-electron effect of the indole moiety.[11] The indole moiety must be located near the methoxy group. The methoxy group could not be assigned.

Fluorescence spectra of aqueous solutions of (*S*)-Trp-O-Pr$^+$ (Cl^-) and (*S*)-Trp-(*S*)-Trp-O-*i*Pr$^+$ (Cl^-) were measured at 25°C (Fig. 7). Further, after adding MeCel2 to each solution, fluorescence spectra were measured. Under equal quantities

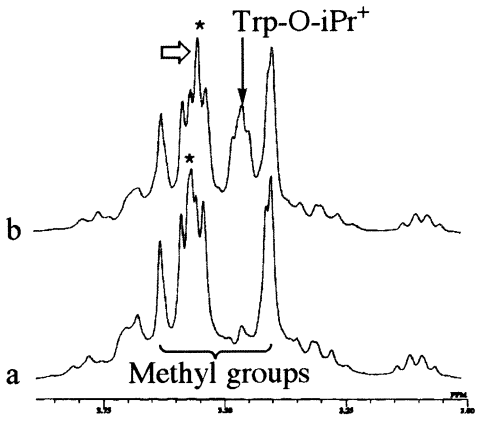

Figure 6. Methyl protons in ^{1}H-NMR spectra of MeCel2 in D_2O at 298K: (a) β-MeCel2 only; (b) β-MeCel2+Trp-O-*i*Pr$^+$(Cl^-), [Trp-O-*i*Pr$^+$]/[β-MeCel2]=*ca.* 15. One methyl proton (*) showed high-field shift (0.02 ppm).

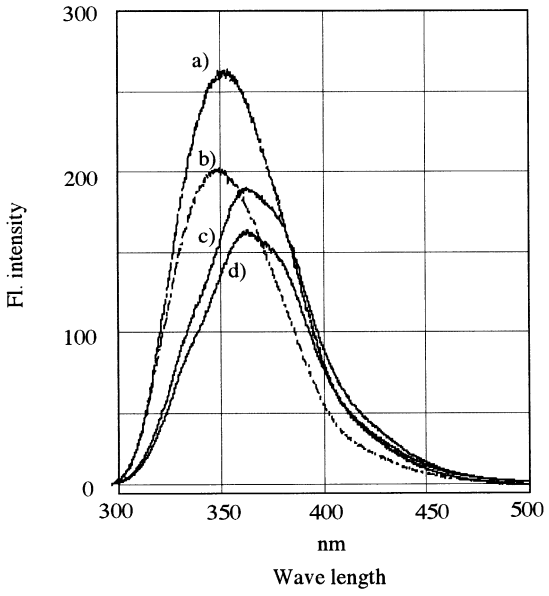

Figure 7. Fluorescence spectra of (*S*)-Trp-O-*i*Pr$^+$ and (*S*)-Trp-(*S*)-Trp-O-*i*Pr$^+$ in H_2O at 298 K. The exciting wavelength was 287 nm: (a) (*S*)-Trp-O-*i*Pr$^+Cl^-$, $[A^+Cl^-]=3.53\times10^{-5}$ M; (b) (*S*)-Trp-O-*i*Pr$^+Cl^-$+β-MeCel2, [S]/$[A^+Cl^-]$=50 (mol/mol); (c) (*S*)-Trp-(*S*)-Trp-O-*i*Pr$^+$, $[A^+Cl^-]=3.87\times10^{-5}$ M; (d) (*S*)-Trp-(*S*)-Trp-O-*i*Pr$^+$+β-MeCel2, [S]/$[A^+Cl^-]$=100 (mol/mol).

of the same amino acid units, the fluorescence intensity of the dipeptide ester salt was smaller than that of the monoamino acid ester salt because the exciting energy of the indole moieties was quenched by the π–π intramolecular interaction between the indole moietes.[12] By adding an excess of MeCel2 to (*S*)-Trp-O-Pr$^+$ (Cl^-) solution, the fluorescence intensity was reduced by about 25% on the anisotropy effect. By adding the same amount of MeCel2 to (*S*)-Trp-(*S*)-Trp-O-*i*Pr$^+$ (Cl^-), the intensity was reduced by about 14%. This reduction of the fluorescence intensity suggests that the quenching became weaker during the intermolecular interaction between the indole moieties and β-MeCel2, which inhibits the intramolecular stacking of the indole moieties in (*S*)-Trp-(*S*)-Trp-O-*i*Pr$^+$ (Cl^-). In the case of β-MeCD, which has the larger association ability toward electrophobic compounds in water,[13] the fluorescence intensity was enhanced by about 15% as the larger inhibition effect on the quenching in the dipeptide. In adding β-MeMal2 instead of β-MeCel2, the reduction of fluorescence intensity of the (*S*)-Trp-O-*i*Pr$^+$ (Cl^-) solution was at the same level as that of the (*S*)-Trp-(*S*)-Trp-O-*i*Pr$^+$ (Cl^-).

From the above results, the mechanism of chiral discrimination found in the action of permethylated cellooligosaccharides toward Trp-O-*i*Pr$^+$ can be accounted for by three interaction concepts described as follows.[14]

1. The ammonium cation moiety in Trp-O-*i*Pr$^+$ binds to the methoxy oxygen (OMe-3) of one glucopyranose moiety (electrostatic interaction).
2. The indole moiety in Trp-O-*i*Pr$^+$ binds to the methoxy group of the next glucopyranose moiety (CH–π interaction).[15]
3. The other substituents of the asymmetric carbon in Trp-O-*i*Pr$^+$ are the 2-propyl ester group and the hydrogen.

In the situation where the 2-propyl ester group locates near part of the permethylated cello-oligosaccharide, the complex becomes unstable with respect to repulsion (steric effects). In the situation where the latter hydrogen locates near part of the permethylated cello-oligosaccharide, the complex becomes more stable. The difference in the stability of these diastereomeric complexes reflects the chiral discrimination toward Trp-O-*i*Pr$^+$. In order to clarify the binding site in more detail, further investigations must be undertaken by means of X-ray crystallography because of the small interactions between the given permethylated oligosaccharides and amino acid ester salts.

3. Summary

We clarified that permethylated oligosaccharides consisting of only a glucopyranose ring unit show various levels of chiral discrimination toward the present amino acid ester salts depending on the number of the units and the glycosyl link style such as α(1→4), β(1→4), β(1→3), and α(1→6). For example, the present permethylated cello-oligosaccharides of the β(1→4) bond form showed different chiral discriminations toward tryptophan derivatives from the present permethylated malto-oligosaccharides of the α(1→4) bond form. The reasons are that the structures and the binding sites of the oligosaccharides are very different from each other as is presumed using NMR, FL spectral and MD calculation methods. It was assumed that series I structures have the same binding behavior as that found with the permethylated cyclodextrins, and that series II molecules have a binding site which consists of two adjacent glucopyranose moieties in a linear-type structure.

In monosaccharides, there are many epimers such as glucose, galactose, mannose, etc. The oligosaccharides suitably consisting of epimers must show a strongly different chiral or molecular discrimination ability.

4. Experimental

4.1. Materials

Permethylated oligosaccharides: the present permethylated oligosaccharides were prepared from free oligosaccharides (hydroxyl type) by the Hakomori method.[16] The commercial products were used in the cases of malto-oligosaccharides (Hayashihara Biochemical Laboratories, Inc.), cello-oligosaccharides (Sigma), and isomalto-oligosaccharides (Seikagaku Corporation). Laminari-oligosaccharides were synthesized by an enzyme reaction.[17] The prepared permethylated oligosaccharides were purified using medium-pressure liquid chromatography (silica gel 60, AcOEt/*n*-hexane/MeOH=5:5:1 by volume) to the anomers, respectively. Isomalto-oligosaccharides could not be purified to the anomers. Note that the anomeric mixtures were used in these experiments.

Physical and spectral properties of the permethylated *gluco*-oligosaccharides are presented in the following sections.

4.2. Series I

4.2.1. β-MeMal2. Colorless syrup; ^{1}H-NMR (300 MHz, $CDCl_3$) δ (ppm) 5.64 (d, 1H, $^3J_{1,2}$=3.9 Hz, H1α-B), 4.15 (d, 1H, $^3J_{1,2}$=7.7 Hz, H1β-A), 3.83 (dd, 1H, $^3J_{3,4}$=8.8 Hz, $^3J_{4,5}$=9.7 Hz, H4-A), 3.64 (s, 3H, —CH_3), 3.56 (s, 3H, —CH_3), 3.55 (s, 3H, —CH_3), 3.54 (s, 6H, —CH_3), 3.53 (s, 3H, —CH_3), 3.40 (s, 3H, —CH_3), 3.33 (s, 3H, —CH_3), 3.60–3.37 (m, 16H, pyranose ring protons), 3.42 (dd, 1H, $^3J_{2,3}$=9.5 Hz, $^3J_{3,4}$=9.0 Hz, H3-B), 3.41 (dd, 1H, $^3J_{2,3}$=9.2 Hz, $^3J_{3,4}$=8.8 Hz, H3-A), 3.26 (dd, 1H, $^3J_{3,4}$=8.8 Hz, $^3J_{4,5}$=9.9 Hz, H4-B), 3.19 (dd, 1H, $^3J_{1,2}$=3.9 Hz, $^3J_{2,3}$=9.7 Hz, H4-B), 3.06 (dd, 1H, $^3J_{1,2}$=7.8 Hz, $^3J_{2,3}$=9.2 Hz, H4-A) from TMS. FT-IR (neat, cm^{-1}) 1186, 1146, 1030 (ether).

4.2.2. β-MeMal3. Colorless syrup; ^{1}H-NMR (300 MHz, $CDCl_3$) δ (ppm) 5.64 (d, 1H, $^3J_{1,2}$=3.7 Hz, H1α), 5.54 (d, 1H, $^3J_{1,2}$=3.9 Hz, H1α), 4.16 (d, 1H, $^3J_{1,2}$=7.7 Hz, H1β), 3.62 (s, 3H, —CH_3), 3.57 (s, 3H, —CH_3), 3.56 (s, 3H, —CH_3), 3.55 (s, 6H, —CH_3), 3.54 (s, 3H, —CH_3), 3.53 (s, 6H, —CH_3), 3.51 (s, 3H, —CH_3), 3.40 (s, 3H, —CH_3), 3.35 (s, 3H, —CH_3), 3.32 (s, 3H, —CH_3), 3.60–3.06 (m, 18H, pyranose ring protons) from TMS. FT-IR (neat, cm^{-1}) 1186, 1148, 1102, 1040 (ether). FABMS (NBA matrix) *m*/*z* 697 $(M+K)^+$.

4.2.3. β-MeMal4. Colorless syrup; ^{1}H-NMR (300 MHz, $CDCl_3$) δ (ppm) 5.65 (d, 1H, $^3J_{1,2}$=3.8 Hz, H1α), 5.56 (d, 1H, $^3J_{1,2}$=3.9 Hz, H1α), 5.54 (d, 1H, $^3J_{1,2}$=3.7 Hz, H1α), 4.17 (d, 1H, $^3J_{1,2}$=7.7 Hz, H1β), 3.61 (s, 3H, —CH3), 3.58 (s, 3H, —CH3), 3.57 (s, 3H, —CH3), 3.56 (s, 6H, —CH3), 3.55 (s, 3H, —CH3), 3.54 (s, 3H, —CH3), 3.53 (s, 3H, —CH3), 3.52 (s, 3H, —CH3), 3.51 (s, 3H, —CH3), 3.49 (s, 3H, —CH3), 3.36 (s, 3H, —CH3), 3.35 (s, 3H, —CH3), 3.30 (s, 3H, —CH3), 3.26 (s, 3H, —CH3), 3.60–3.02 (m, 24H, pyranose ring protons) from TMS. FT-IR (neat, cm^{-1}) 1188, 1151, 1102, 1042 (ether). FABMS (NBA matrix) *m*/*z* 1001 $(M+K)^+$.

4.2.4. β-MeMal5. Colorless syrup; ^{1}H-NMR (300 MHz, $CDCl_3$) δ (ppm) 5.64 (d, 1H, $^3J_{1,2}$=3.7 Hz, H1α), 5.57 (d, 1H, $^3J_{1,2}$=3.9 Hz, H1α), 5.56 (d, 1H, $^3J_{1,2}$=3.0 Hz, H1α), 5.53 (d, 1H, $^3J_{1,2}$=3.9 Hz, H1α), 4.17 (d, 1H, $^3J_{1,2}$=7.7 Hz, H1β), 3.61 (s, 3H, —CH_3), 3.57 (s, 3H, —CH_3), 3.56 (s, 3H, —CH_3), 3.55 (s, 6H, —CH_3), 3.55 (s, 3H, —CH_3), 3.54 (s, 3H, —CH_3), 3.53 (s, 3H, —CH_3), 3.52 (s, 3H, —CH_3), 3.51 (s, 3H, —CH_3), 3.50 (s, 3H, —CH_3), 3.46 (s, 3H, —CH_3), 3.31 (s, 3H, —CH_3), 3.30 (s, 3H, —CH_3), 3.27 (s, 3H, —CH_3), 3.60–3.02 (m, 30H, pyranose ring protons) from TMS. FT-IR (neat, cm^{-1}) 1151, 1102, 1026 (ether). FABMS (NBA matrix) *m*/*z* 1105 $(M+K)^+$.

4.2.5. β-MeMal6. Colorless syrup; ^{1}H-NMR (300 MHz, $CDCl_3$) δ (ppm) 5.65 (d, 1H, $^3J_{1,2}$=3.7 Hz, H1α), 5.58 (d, 1H, $^3J_{1,2}$=3.5 Hz, H1α), 5.57 (d, 1H, $^3J_{1,2}$=4.0 Hz, H1α), 5.56 (d, 1H, $^3J_{1,2}$=3.9 Hz, H1α), 5.53 (d, 1H, $^3J_{1,2}$=3.7 Hz, H1α), 4.17 (d, 1H, $^3J_{1,2}$=7.7 Hz, H1β), 3.61 (s, 3H, —CH_3), 3.59 (s, 3H, —CH_3), 3.58 (s, 3H, —CH_3), 3.57 (s, 6H, —CH_3), 3.56 (s, 3H, —CH_3), 3.56 (s, 3H, —CH_3), 3.55 (s, 3H, —CH_3), 3.54 (s, 3H, —CH_3), 3.53 (s, 3H, —CH_3), 3.52 (s, 3H, —CH_3), 3.52 (s, 3H, —CH_3), 3.51 (s, 3H, —CH_3), 3.50 (s, 3H, —CH_3), 3.40 (s, 3H, —CH_3), 3.40 (s, 3H,

—CH_3), 3.39 (s, 3H, —CH_3), 3.36 (s, 3H, —CH_3), 3.34 (s, 3H, —CH_3), 3.31 (s, 3H, —CH_3), 3.60–3.02 (m, 36H, pyranose ring protons) from TMS. FT-IR (neat, cm^{-1}) 1188, 1156, 1102, 1038 (ether). FABMS (NBA matrix) *m/z* 1309 $(M+K)^+$.

4.2.6. β-MeMal7. Colorless syrup; ^{1}H-NMR (300 MHz, $CDCl_3$) δ (ppm) 5.65 (d, 1H, $^3J_{1,2}$=3.7 Hz, H1α), 5.58–5.57 (d, 4H, $^3J_{1,2}$=3.5 Hz, H1α), 5.53 (d, 1H, $^3J_{1,2}$=4.0 Hz, H1α), 4.17 (d, 1H, $^3J_{1,2}$=7.9 Hz, H1β), 3.61 (s, 3H, —CH_3), 3.59 (s, 3H, —CH_3), 3.57 (s, 3H, —CH_3), 3.57 (s, 6H, —CH_3), 3.56 (s, 3H, —CH_3), 3.55 (s, 3H, —CH_3), 3.54 (s, 3H, —CH_3), 3.53 (s, 3H, —CH_3), 3.53 (s, 3H, —CH_3), 3.52 (s, 3H, —CH_3), 3.52 (s, 3H, —CH_3), 3.51 (s, 3H, —CH_3), 3.51 (s, 3H, —CH_3), 3.50 (s, 3H, —CH_3), 3.40 (s, 3H, —CH_3), 3.40 (s, 3H, —CH_3), 3.39 (s, 3H, —CH_3), 3.39 (s, 3H, —CH_3), 3.35 (s, 3H, —CH_3), 3.33 (s, 3H, —CH_3), 3.31 (s, 3H, —CH_3), 3.60–3.02 (m, 42H, pyranose ring protons) from TMS. FT-IR (neat, cm^{-1}) 1188, 1156, 1102, 1024 (ether). FABMS (NBA matrix) *m/z* 1467 $(M+K)^+$.

4.3. Series II

4.3.1. β-MeCel2. Colorless crystal; mp=75–76°C; ^{1}H-NMR (300 MHz, $CDCl_3$) δ (ppm) 4.31 (d, 1H, $^3J_{1,2}$=7.9 Hz, H1(β)), 4.15 (d, 1H, $^3J_{1,2}$=7.7 Hz, H1(β)), 3.71–3.11(m, 10H, pyranose ring protons), 3.62 (s, 3H, —CH_3), 3.58 (s, 3H, —CH_3), 3.57 (s, 3H, —CH_3), 3.55 (s, 3H, —CH_3), 3.53 (s, 3H, —CH_3), 3.52 (s, 3H, —CH_3), 3.48 (s, 3H, —CH_3), 3.62 (s, 3H, —CH_3), 3.40 (s, 3H, —CH_3), 3.39 (s, 3H, —CH_3), 3.02 (t, 1H, $^3J_{1,2}$=$^3J_{2,3}$=8.1 Hz, H2), 2.93 (t, 3H, 1H, $^3J_{1,2}$=$^3J_{2,3}$=8.1 Hz, H2) from TMS. FT-IR (KBr disk, cm^{-1}) 1132, 1100, 1067, 1044 (ether). FABMS (NBA matrix) *m/z* 493 $(M+K)^+$.

4.3.2. β-MeCel3. Colorless crystal; mp=106–108°C; ^{1}H-NMR (300 MHz, $CDCl_3$) δ (ppm) 4.32 (d, 2H, $^3J_{1,2}$=7.9 Hz, H1(β)), 4.15 (d, 1H, $^3J_{1,2}$=7.7 Hz, H1(β)), 3.79–3.10 (m, 15H, pyranose ring protons), 3.62 (s, 3H, —CH_3), 3.58 (s, 3H, —CH_3), 3.57 (s, 3H, —CH_3), 3.55 (s, 3H, —CH_3), 3.54 (s, 3H, —CH_3), 3.52 (s, 3H, —CH_3), 3.40 (s, 3H, —CH_3), 3.62 (s, 3H, —CH_3), 3.39 (s, 3H, —CH_3), 3.38 (s, 3H, —CH_3), 3.02 (t, 1H, $^3J_{1,2}$=$^3J_{2,3}$=7.9 Hz, H2), 2.97 (t, 1H, $^3J_{1,2}$=$^3J_{2,3}$=8.1 Hz, H2), 2.93 (t, 3H, 1H, $^3J_{1,2}$=$^3J_{2,3}$=6.7 Hz, H2) from TMS. FT-IR (KBr disk, cm^{-1}) 1142, 1124, 1090, 1042 (ether). FABMS (NBA matrix) *m/z* 697 $(M+K)^+$.

4.3.3. β-MeCel4. Colorless crystal; mp=116–118°C; ^{1}H-NMR (300 MHz, $CDCl_3$) δ (ppm) 4.33 (d, 1H, $^3J_{1,2}$=7.5 Hz, H1(β)), 4.32 (d, 2H, $^3J_{1,2}$=7.9 Hz, H1(β)), 4.15 (d, 1H, $^3J_{1,2}$=7.7 Hz, H1(β)), 3.92–2.80 (m, 24H, pyranose ring protons), 3.62 (s, 3H, —CH_3), 3.58 (s, 3H, —CH_3), 3.55 (s, 3H, —CH_3), 3.54 (s, 3H, —CH_3), 3.52 (s, 3H, —CH_3), 3.41 (s, 3H, —CH_3), 3.40 (s, 3H, —CH_3), 3.39 (s, 3H, —CH_3) from TMS. FT-IR (KBr disk, cm^{-1}) 1126, 1090, (ether). FABMS (NBA matrix) *m/z* 901 $(M+K)^+$.

4.3.4. β-MeCel5. Colorless crystal; mp=134–135°C; ^{1}H-NMR (300 MHz, $CDCl_3$) δ (ppm) 4.33 (d, 2H, $^3J_{1,2}$=7.7 Hz, H1(β)), 4.32 (d, 2H, $^3J_{1,2}$=7.7 Hz, H1(β)), 4.15 (d, 1H, $^3J_{1,2}$=7.7 Hz, H1(β)), 3.79–2.92 (m, 30H, pyranose ring protons), 3.62 (s, 3H, —CH_3), 3.58 (s, 3H, —CH_3), 3.55 (s, 3H, —CH_3), 3.54 (s, 3H, —CH_3), 3.52 (s, 3H, —CH_3), 3.40 (s, 3H, —CH_3), 3.39 (s, 3H, —CH_3) from TMS. FT-IR (KBr disk, cm^{-1}) 1068 (ether). FABMS (NBA matrix) *m/z* 1105 $(M+K)^+$.

4.4. Series III-α

4.4.1. α-MeLam2. Colorless syrup; ^{1}H-NMR (300 MHz, $CDCl_3$) δ (ppm) 4.84 (d, 1H, $^3J_{1,2}$=3.5 Hz, H1), 4.69 (d, 1H, $^3J_{1,2}$=7.7 Hz, H1), 4.08 (t, 1H, $^3J_{2,3}$=$^3J_{3,4}$=9.0 Hz, H3), 3.60–3.13 (m, 9H, pyranose ring protons), 3.62 (s, 3H, —CH_3), 3.59 (s, 3H, —CH_3), 3.53 (s, 3H, —CH_3), 3.52 (s, 3H, —CH_3), 3.48 (s, 3H, —CH_3), 3.42 (s, 3H, —CH_3), 3.41 (s, 3H, —CH_3), 3.40 (s, 3H, —CH_3) 3.29 (dd, 1H, $^3J_{1,2}$=3.5 Hz, $^3J_{2,3}$=9.5 Hz, H2), 2.99–2.91 (m, 1H, pyranose ring proton) from TMS. FT-IR (neat, cm^{-1}) 1102, 1051 (ether). FABMS (NBA matrix) *m/z* 493 $(M+K)^+$.

4.4.2. α-MeLam3. Colorless syrup; ^{1}H-NMR (300 MHz, $CDCl_3$) δ (ppm) 4.84 (d, 1H, $^3J_{1,2}$=3.5 Hz, H1), 4.69 (d, 1H, $^3J_{1,2}$=7.9 Hz, H1), 4.69 (d, 1H, $^3J_{1,2}$=8.0 Hz, H1), 4.08 (t, 1H, $^3J_{2,3}$=$^3J_{3,4}$=9.0 Hz, H3), 3.77–3.65 (m, 2H, pyranose ring protons), 3.63 (s, 3H, —CH_3), 3.61 (s, 3H, —CH_3), 3.58 (s, 3H, —CH_3), 3.54 (s, 3H, —CH_3), 3.52 (s, 3H, —CH_3), 3.51 (s, 3H, —CH_3), 3.48 (s, 3H, —CH_3), 3.41 (s, 3H, —CH_3), 3.40 (s, 3H, —CH_3), 3.63–2.96 (m, 15H, pyranose ring proton) from TMS. FT-IR (neat, cm^{-1}) 1100, 1053 (ether). FABMS (NBA matrix) *m/z* 697 $(M+K)^+$.

4.4.3. α-MeLam4. Colorless syrup; ^{1}H-NMR (300 MHz, $CDCl_3$) δ (ppm) 4.84 (d, 1H, $^3J_{1,2}$=3.4 Hz, H1), 4.69 (d, 1H, $^3J_{1,2}$=7.5 Hz, H1), 4.68 (d, 1H, $^3J_{1,2}$=7.9 Hz, H1), 4.68 (d, 1H, $^3J_{1,2}$=8.1 Hz, H1), 4.08 (t, 1H, $^3J_{2,3}$=$^3J_{3,4}$= 9.2 Hz, H3), 3.63–3.40 (m, 2H, pyranose ring protons), 3.63 (s, 3H, —CH_3), 3.61 (s, 3H, —CH_3), 3.58 (s, 3H, —CH_3), 3.54 (s, 3H, —CH_3), 3.52 (s, 3H, —CH_3), 3.51 (s, 3H, —CH_3), 3.48 (s, 3H, —CH_3), 3.41 (s, 3H, —CH_3), 3.41 (s, 3H, —CH_3), 3.40 (s, 3H, —CH_3), 3.32–2.93 (m, 20H, pyranose ring proton) from TMS. FT-IR (neat, cm^{-1}) 1127, 1053, 1053 (ether). FABMS (NBA matrix) *m/z* 901 $(M+K)^+$.

4.4.4. α-MeLam5. Colorless syrup; ^{1}H-NMR (300 MHz, $CDCl_3$) δ (ppm) 4.84 (d, 1H, $^3J_{1,2}$=3.3 Hz, H1), 4.70 (d, 2H, $^3J_{1,2}$=7.7 Hz, H1), 4.69 (d, 2H, $^3J_{1,2}$=7.7 Hz, H1), 4.08 (t, 1H, $^3J_{2,3}$=$^3J_{3,4}$=9.2 Hz, H3), 3.78–2.89 (m, 29H, pyranose ring protons), 3.63 (s, 3H, —CH_3), 3.60 (s, 3H, —CH_3), 3.58 (s, 3H, —CH_3), 3.55 (s, 3H, —CH_3), 3.52 (s, 3H, —CH_3), 3.48 (s, 3H, —CH_3), 3.40 (s, 3H, —CH_3) from TMS. FT-IR (neat, cm^{-1}) 1100, 1055 (ether). FABMS (NBA matrix) *m/z* 1105 $(M+K)^+$.

4.5. Series III-β

4.5.1. β-MeLam2. Colorless syrup; ^{1}H-NMR (300 MHz, $CDCl_3$) δ (ppm) 4.68 (d, 1H, $^3J_{1,2}$=7.7 Hz, H1), 4.13 (d, 1H, $^3J_{1,2}$=7.9 Hz, H1), 3.76 (t, 1H, $^3J_{2,3}$=$^3J_{3,4}$=8.8 Hz, H3), 3.67–3.14 (m, 9H, pyranose ring protons), 3.63 (s, 3H, —CH_3), 3.59 (s, 3H, —CH_3), 3.57 (s, 3H, —CH_3), 3.52 (s, 3H, —CH_3), 3.40 (s, 3H, —CH_3), 3.07 (dd, 1H,

$^3J_{2,3}$=$^3J_{3,4}$=8.4 Hz, H3), 2.93 (m, 1H, pyranose ring proton) from TMS. FT-IR (neat, cm^{-1}) 1107, 1059 (ether). FABMS (NBA matrix) *m/z* 493 $(M+K)^+$.

4.5.2. β-MeLam3. Colorless syrup; ^{1}H-NMR (300 MHz, $CDCl_3$) δ (ppm) 4.69 (d, 1H, $^3J_{1,2}$=7.7 Hz, H1), 4.69 (d, 1H, $^3J_{1,2}$=8.1 Hz, H1), 4.14 (d, 1H, $^3J_{1,2}$=8.1 Hz, H1), 3.77 (t, 1H, $^3J_{2,3}$=$^3J_{3,4}$=8.8 Hz, H3), 3.74 (t, 1H, $^3J_{2,3}$=$^3J_{3,4}$=7.3 Hz, H3), 3.67–3.15 (m, 13H, pyranose ring protons), 3.63 (s, 3H, —CH_3), 3.61 (s, 3H, —CH_3), 3.59 (s, 3H, —CH_3), 3.55 (s, 3H, —CH_3), 3.52 (s, 3H, —CH_3), 3.40 (s, 3H, —CH_3), 3.07 (t, 1H, $^3J_{2,,3}$=$^3J_{3,4}$=8.8 Hz, H3), 3.02 (t, 1H, $^3J_{2,,3}$=$^3J_{3,4}$=8.8 Hz, H3), 2.93 (m, 1H, pyranose ring proton) from TMS. FT-IR (neat, cm^{-1}) 1105, 1059 (ether). FABMS (NBA matrix) *m/z* 697 $(M+K)^+$.

4.5.3. β-MeLam4. Colorless syrup; ^{1}H-NMR (300 MHz, $CDCl_3$) δ (ppm) 4.70 (d, 1H, $^3J_{1,2}$=7.7 Hz, H1), 4.69 (d, 2H, $^3J_{1,2}$=7.9 Hz, H1), 4.13 (d, 1H, $^3J_{1,2}$=7.9 Hz, H1), 3.75 (t, 1H, $^3J_{2,3}$=$^3J_{3,4}$=8.8 Hz, H3), 3.65–3.43 (m, 9H, pyranose ring protons), 3.63 (s, 3H, —CH_3), 3.61 (s, 3H, —CH_3), 3.60 (s, 3H, —CH_3), 3.59 (s, 3H, —CH_3), 3.55 (s, 3H, —CH_3), 3.52 (s, 3H, —CH_3), 3.40 (s, 3H, —CH_3), 3.40 (s, 3H, —CH_3), 3.36–2.90 (m, 1H, pyranose ring proton) from TMS. FT-IR (neat, cm^{-1}) 1107, 1057 (ether). FABMS (NBA matrix) *m/z* 901 $(M+K)^+$.

4.5.4. β-MeLam5. Colorless syrup; ^{1}H-NMR (300 MHz, $CDCl_3$) δ (ppm) 4.70 (d, 1H, $^3J_{1,2}$=7.7 Hz, H1), 4.69 (d, 2H, $^3J_{1,2}$=7.7 Hz, H1), 4.13 (d, 1H, $^3J_{1,2}$=7.9 Hz, H1), 3.75 (m, 4H, pyranose ring protons), 3.62–3.40 (m, 1H, pyranose ring protons), 3.63 (s, 3H, —CH_3), 3.61 (s, 3H, —CH_3), 3.60 (s, 3H, —CH_3), 3.59 (s, 3H, —CH_3), 3.56 (s, 3H, —CH_3), 3.52 (s, 3H, —CH_3), 3.50 (s, 3H, —CH_3), 3.48 (s, 3H, —CH_3), 3.41 (s, 3H, —CH_3), 3.31–2.90 (m, 16H, pyranose ring proton) from TMS. FT-IR (neat, cm^{-1}) 1098, 1055 (ether). FABMS (NBA matrix) *m/z* 1105 $(M+K)^+$.

4.6. Series IV: anomeric mixture

4.6.1. MeImal2. Colorless solid; ^{1}H-NMR (300 MHz, $CDCl_3$) δ (ppm) 5.03 (d, $^3J_{1,2}$=3.1 Hz, reducing terminal proton H1α), 4.96 (d, 1H, $^3J_{1,2}$=3.1 Hz, H1α), 4.13 (d, $^3J_{1,2}$=7.8 Hz, reducing terminal proton H1β) from TMS, α/β ratio=1/0.28; FT-IR (KBr disk, cm^{-1}) 1108, 1068 (ethers).

4.6.2. MeImal3. Colorless solid; ^{1}H-NMR (300 MHz, $CDCl_3$) δ (ppm) 5.03 (d, $^3J_{1,2}$=3.0 Hz, reducing terminal proton H1α), 4.97 (d, 2H, $^3J_{1,2}$=3.0 Hz, H1α), 4.13 (d, $^3J_{1,2}$=7.5 Hz, reducing terminal proton H1β) from TMS, α/β ratio=1/0.23; FT-IR (KBr disk, cm^{-1}) 1140, 1102, 1040 (ethers).

4.6.3. MeImal4. Colorless solid; ^{1}H-NMR (300 MHz, $CDCl_3$) δ (ppm) 5.03 (d, $^3J_{1,2}$=3.1 Hz, reducing terminal proton H1α), 4.97 (d, 3H, $^3J_{1,2}$=3.1 Hz, H1α), 4.14 (d, $^3J_{1,2}$=7.5 Hz, reducing terminal proton H1β) from TMS, α/β ratio=1/0.25; FT-IR (KBr disk, cm^{-1}) 1102, 1042 (ethers).

4.6.4. MeImal5. Colorless solid; ^{1}H-NMR (300 MHz, $CDCl_3$) δ (ppm) 5.03 (d, $^3J_{1,2}$=3.1 Hz, reducing terminal proton H1α), 4.96 (d, 4H, $^3J_{1,2}$=3.0 Hz, H1α), 4.12 (d, $^3J_{1,2}$=7.8 Hz, reducing terminal proton H1β) from TMS, α/β ratio=1/0.23; FT-IR (KBr disk, cm^{-1}) 1159, 1102, 1041 (ethers).

4.6.5. MeImal6. Colorless solid; ^{1}H-NMR (300 MHz, $CDCl_3$) δ (ppm) 5.03 (d, $^3J_{1,2}$=3.2 Hz, reducing terminal proton H1α), 4.96 (d, 5H, $^3J_{1,2}$=3.0 Hz, H1α), 4.13 (d, $^3J_{1,2}$=7.8 Hz, reducing terminal proton H1β) from TMS, α/β ratio=1/0.24; FT-IR (KBr disk, cm^{-1}) 1174, 1016.

4.6.6. MeImal7. Colorless solid; ^{1}H-NMR (300 MHz, $CDCl_3$) δ (ppm) 5.03 (d, $^3J_{1,2}$=3.2 Hz, reducing terminal proton H1α), 4.96 (d, 6H, $^3J_{1,2}$=3.0 Hz, H1α), 4.13 (d, $^3J_{1,2}$=7.5 Hz, reducing terminal proton H1β) from TMS, α/β ratio=1/0.22; FT-IR (KBr disk, cm^{-1}) 1108, 1096, 1044, 1028.

4.7. Further materials

Amino acid 2-propyl ester hydrochlorides: the present amino acid 2-propyl ester hydrochlorides were prepared by the esterification of the free amino acids with 2-propanol under HCl catalyst.[18] (*S*)-Enantiomers were reacted with deuterium-labeled 2-propanol (99 at.% D, CDN isotopes). (*R*)-Enantiomers were reacted with unlabeled 2-propanol (Wako).

(S)-Trp-(S)-Trp-O-iPr$^+$(Cl$^-$): equimolar Boc-(*S*)-Trp and (*S*)-Trp-O-*i*Pr$^+$ were dissolved in DMF containing 1.1 equimolar triethylamine and HOBt and the mixture condensed with equimolar 1-(3-dimethylaminopropyl)-3-ethylcarbodiimide hydrochloride (EDC).[19] After cleavage of the protective group with TFA, the counter anion was exchanged with Cl^- using an anion-exchange resin (Dowex AG1-X2, Cl^- form). The product was recrystallized in MeOH/AcOEt to yield 54% product. ^{1}H-NMR (300 MHz, DMSO) δ (ppm) 11.03 (s, 1H, NH), 7.72 (d, 1H, ^3J=7.5 Hz, —C—C*H*=CH), 7.52 (d, 1H, ^3J=6.8 Hz, —C—C*H*=CH), 7.38 (d, 1H, ^3J=7.8 Hz, —C—CH=C*H*), 7.35 (d, 1H, ^3J=6.9 Hz, C—CH=C*H*), 7.25–6.98 (m, 6H, aromatic protons), 4.84 (m, 1H, C*H*—NH_2^+), 4.60 (m, 1H, C*H*—NH_3^+), 4.03 (m, 1H, —C*H*(CH_3)$_2$), 3.20–3.10 (m, 4H, methylene), 1.15 (d, 3H, ^3J=6.1 Hz, —CH(C*H*$_3$)$_2$), 1.01 (d, 3H, ^3J=6.6 Hz, —CH(C*H*$_3$)$_2$) from TMS.

4.8. General

FAB mass spectra were measured with a JEOL SX-102 mass spectrometer and the data were analyzed with a JMA-DA 6000 data processing system. NMR spectra were measured with a JEOL AL-300 spectrometer. FL spectra were measured with a Shimadzu RF-5300PC fluorescence photometer.

Synthesized compounds were assigned using other instrumental analyses (FT-IR: Shimadzu FT-IR 8100 spectrometer; elemental analysis: Perkin–Elmer 2400; melting points: Yanaco-MP apparatus).

4.9. FABMS/EL guest method

FAB mass spectra (positive mode) were measured operating at an accelerating voltage of 10 kV with a mass range of *m/z* 100–2400. The instrument was equipped with a standard JEOL FAB source and an ion gun. Xenon was used as the atom beam with an emission current of 10 mA and an acceleration of 3 kV. The ion source pressure was typically ca. $1–2\times10^{-5}$ Torr. Spectra were obtained with a magnet scan rate of 10 s scan^{-1} (to *m/z* 2400) at room temperature (25°C) and the data were processed with a JEOL JMA-DA 6000 data processing system. Calibration was carried out with CsI.

A sample solution was prepared by mixing two solutions and matrix (3-nitrobenzyl alcohol, Aldrich). FAB mass spectra were measured at room temperature with the deposit of a 1 μL aliquot of the mixed solution, which stood overnight to homogenize. The three solutions were as follows: (1) 10 μL of a 1.33 M MeOH solution of a 1/1 mixture of unlabeled (*R*)- and labeled *S*-amino acid ester salts ($[A_R{}^+Cl^-]$=0.67 M and $[A_{S-dn}{}^+Cl^-]$=0.67 M; (2) 5 μL of a 0.20 M $CHCl_3$ solution of a given permethylated oligosaccharide; and (3) 15 μL of NBA matrix. The accuracy of the 1/1 equivalent concentration of (*R*)- and (*S*)-enantiomers of the amino acid ester salts was confirmed from the relative intensity (I_R/I_{S-dx}) values with 18-crown-6 (Tokyo Kasei), which is an achiral host, and was experimentally obtained as unity (1.00±0.03).

Each relative intensity (I_R/I_{S-dx}) value was the average of the experimental values obtained during the 10th, 20th, 30th, and 40th scans. The observed peak intensity of a permethylated oligosaccharide/*S*-amino acid ester complex ion (I_{S-dx}) inevitably contains contributions from the amounts of (M+6) or (M+7) naturally abundant isotopes derived from the peak intensity of a permethylated oligosaccharide/(*R*)-amino acid ester complex ion (I_R). However, the theoretical distribution (%) of the (M+6) or (M+7) isotpes was too small (<1%) to correct.

4.10. Molecular simulation

All molecular model simulations were calculated with a software Cerius^2 (MSI, ver. 4.0) on a Silicon Graphic workstation Unix system (octane). The initial molecular structures were constructed with a 3D-Sketcher software module in Cerius^2 and the molecular structures were optimized with a Molecular Mechanics (force field: PCFF).[20] The molecular dynamics of the permethylated oligosaccharides were simulated using a canonical (NTV) ensemble (*T*=298 K), and the temperature was controlled by the Hoover dynamics method.[21] One step of the calculation is 1 fs. The calculation was repeated over 500,000 steps (500 ps). The properties, which are an averaged molecular length, a radius of gyration, and a self-diffusion coefficient were evaluated from the last 5,000,000 steps (5000 ps).

4.11. NMR titration

^{1}H-NMR spectra were measured using the ^{1}H-NMR titration technique reported before.[9] Commercial acetone-d_6 (Aldrich, 99.5 at.% D) was used as a solvent without purification. TMS was used as internal standard. The K_S values for the complexation equilibrium between β-MeCel2 and ammonium thiocyanate at 25°C (298 K) were determined by the following procedure. To an NMR tube containing a 0.6 mL acetone-d_6 solution of β-MeCel2 (8.65 mM) was added dropwise (0, 5, 10, 15, 20, 25, and 30 μL) an acetone-d_6 solution of ammonium thiocyanate (0.460 mM μL^{-1}) and ^{1}H-NMR spectra were measured in order. To maintain the sample solution at a constant temperature the NMR tube was maintained for 15 min on the probe at 25°C (298 K) before measuring the NMR spectra. The averages of the K_S values estimated from the concentration ratio $[NH_4SCN]/[\beta\text{-MeCel2}]$ and the corresponding shifts of the following proton peaks were adopted. It was assumed that a 1:1 complex is stoichiometrically formed in the solution because of the observation of the 1:1 complex ions in FAB mass spectra. The *K* values were calculated using a general non-linear method.[22]

The induced shift of 0.6 mL of β-MeCel2 in D_2O (Aldrich) was measured adding 10 mg of (*S*)-tryptophan 2-propyl ester hydrochlorides. DSS was used as an internal standard.

4.12. Fluorescence spectrometry

FL spectra were measured while maintaining samples at 25°C with a NESLAB endocal refrigerated circulating bath. The exciting wavelength was 287 nm in the cases of both (*S*)-Trp-O-*i*Pr$^+$(Cl$^-$) and (*S*)-Trp-(*S*)-Trp-O-*i*Pr$^+$(Cl$^-$). The emission was scanned in the range 300–500 nm. Disposable cells made from PMMA were used. The concentrations of the prepared solutions of (*S*)-Trp-O-*i*Pr$^+$(Cl$^-$) and (*S*)-Trp-(*S*)-Trp-O-*i*Pr$^+$(Cl$^-$) were 3.53×10^{-5} M and 2.32×10^{-5} M, respectively. The ratio of the indole units in these solutions was 1.0:1.1. The FL spectra of 3.5 mL solutions were measeured before and after adding a 50-fold molar excess of permethylated oligosaccharides (β-MeCel2, β-MeMal2, and β-MeCD).

References

1. (a) Díhulst, A.; Berbeke, N. *Chirality* **1994**, *6*, 225–229. (b) Yashima, E.; Okamoto, Y. *Bull. Chem. Soc. Jpn.* **1995**, *68*, 3289–3307. (c) Yashima, E.; Yamamoto, C.; Okamoto, Y. *J. Am. Chem. Soc.* **1996**, *118*, 4036–4048. (d) Okamoto, Y.; Yashima, E. *Angew. Chem. Int. Ed. Engl.* **1998**, *37*, 1020–1043.
2. (a) Soini, H.; Stefansson, M.; Riekkola, M.-L.; Novotny, M. V. *Anal. Chem.* **1994**, *66*, 3477–3484. (b) Kano, K.; Minami, K.; Horiguchi, K.; Ishimura, T.; Kodera, M. *J. Chromatogr. A* **1995**, *694*, 307–313. (c) Kano, K.; Negi, S.; Takaoka, R.; Kamo, H.; Kitae, T.; Yamaguchi, M.; Okubo, H.; Hirama, M. *Chem. Lett.* **1997**, 715–716.
3. We have found few reports for the enantioselective formation of 1:1 complexes of linear oligosaccharides with chiral compounds until now. In the case of β-cyclodextrin, see: Rekharsky, M.; Inoue, Y. *J. Am. Chem. Soc.* **2000**, *122*, 4418–4435.
4. Sawada, M.; Shizuma, M.; Takai, Y.; Adachi, H.; Takeda, T.; Uchiyama, T. *Chem. Commun.* **1998**, 1453–1454.

5. (a) Sawada, M.; Takai, Y.; Yamada, H.; Hirayama, S.; Kaneda, T.; Tanaka, T.; Kamada, K.; Mizooku, T.; Takeuchi, S.; Ueno, K.; Hirose, K.; Tobe, Y.; Naemura, K. *J. Am. Chem. Soc.* **1995**, *117*, 7726–7736. (b) Sawada, M. *Mass Spectrom. Rev.* **1997**, *16*, 73–90. (c) Sawada, M. *J. Mass Spectrom. Soc. Jpn.* **1997**, *45*, 439–458. (d) Shizuma, M. *J. Mass. Spectrom. Soc. Jpn.* **1998**, *46*, 211–218.
6. The selectivity of the permethylated inulo-oligosaccharides toward the amino acid ester salts follows. $I_R/I_{S\text{-}dx}>1.0$, R-selectivity; $I_R/I_{S\text{-}dx}=1.0$, non-selectivity; $I_R/I_{S\text{-}dx}<1.0$, S-selectivity.
7. Sawada, M.; Takai, Y.; Yamada, H.; Nishida, J.; Kaneda, T.; Arakawa, R.; Okamoto, M.; Hirose, K.; Tanaka, T.; Naemura, K. *J. Chem. Soc., Perkin Trans. 2* **1998**, 701–710.
8. Lipkowitz, K. B.; Raghothama, S.; Yang, J.-a. *J. Am. Chem. Soc.* **1992**, *114*, 1554–1562.
9. Takai, Y.; Okumura, Y.; Sawada, M.; Takahashi, S.; Siro, M.; Kawamura, M.; Uchiyama, T. *J. Org. Chem.* **1994**, *59*, 2967–2975.
10. Live, D.; Chan, S. I. *J. Am. Chem. Soc.* **1976**, *98*, 3769.
11. (a) Nishio, M. *Tetrahedron* **1995**, *51*, 8665. (b) Nishio, M. *Bull. Chem. Soc. Jpn.* **1998**, *71*, 1207.
12. Suzuki, Y.; Morozumi, T.; Nakamura, H.; Shimomura, M.; Hayashita, T.; Bartsh, R. A. *J. Phys. Chem. B* **1998**, *102*, 7910–7917.
13. Otsuki, J.; Kobayashi, K.; Toi, H.; Aoyama, Y. *Tetrahedron Lett.* **1993**, *34*, 1945–1948.
14. Pirkle, W. H.; Pochapsky, T. C. *Chem. Rev.* **1989**, *89*, 347–362.
15. Nishio, M.; Hirota, M. *Tetrahedron* **1989**, *45*, 7201.
16. (a) Hakomori, S. *J. Biochem. (Tokyo)* **1964**, *55*, 205–208. (b) Conard, H. E. In *Method in Carbohydrate Chemistry*; Whister, R. L., Bemiller, S. N., Eds.; Academic Press: New York, 1972; 6, pp 361. (c) Melton, L. D.; McNeil, M.; Darvill, A. G.; Albersheim, P.; Dell, A. *Carbohydr. Res.* **1986**, *146*, 279.
17. Amemura, A.; Moori, K.; Harada, T. *Biochim. Biophys. Acta* **1974**, *334*, 398–409.
18. Kyba, E. P.; Timko, J. M.; Kaplan, L. J.; de Jong, F.; Gokel, G. W.; Cram, D. J. *J. Am. Chem. Soc.* **1978**, *100*, 4555–4568.
19. Todd, J. S.; Proteau, P. J.; Gerwick, W. H. *Tetrahedron Lett.* **1993**, *34*, 7685–7688.
20. Sun, H.; Ren, P.; Fried, J. P. *Computational and Theoretical Polymer Science* **1998**, 229–246.
21. Hoover, W. G. *Computational Statistical Mechanics*, Elsevier: Amsterdam, 1990.
22. (a) Tone, K. In *BASIC*, Baifukan, 1981; pp 137–146 chap. 28. (b) Tsukube, H.; Sohmiya, H. *J. Org. Chem.* **1991**, *56*, 875.